Green Chemistry

PAPER

View Article Online
View Journal | View Issue

Cite this: *Green Chem.*, 2016, **18**, 3835

Highly thermal-stable and functional cellulose nanocrystals and nanofibrils produced using fully recyclable organic acids†

Liheng Chen,[a,b] J. Y. Zhu,*[b] Carlos Baez,[b] Peter Kitin[b] and Thomas Elder[c]

Received 9th March 2016,
Accepted 6th April 2016

DOI: 10.1039/c6gc00687f

www.rsc.org/greenchem

Here we report the production of highly thermal stable and functional cellulose nanocrystals (CNC) and nanofibrils (CNF) by hydrolysis using concentrated organic acids. Due to their low water solubility, these solid organic acids can be easily recovered after hydrolysis reactions through crystallization at a lower or ambient temperature. When dicarboxylic acids were used, the resultant CNC surface contained carboxylic acid groups which facilitate functionalization and dispersion in aqueous processing. The carboxylic acid group content was 0.1–0.4 mmol g^{-1} for CNC produced from a bleached eucalyptus kraft pulp (BEP) using oxalic acid at concentrations of 50–70 wt%. The onset thermal degradation temperature for the CNC was increased to 322 °C from 274 °C for the feed BEP fibers, compared with 218 °C for CNC produced from the same feed fibers using conventional concentrated sulfuric acid hydrolysis. The low strength (high pK_a) of organic acids also resulted in CNC with longer lengths of approximately 275–380 nm and higher crystallinity than those produced using mineral acids. Fibrous cellulosic solid residue (FCSR) collected from acid hydrolysis was an excellent feedstock for producing CNF through subsequent mechanical fibrillation with low energy input. The ability to recover organic acids using a conventional and commercially proven crystallization method makes these organic acids uniquely suitable for sustainable and green production of cellulose nanomaterials. The resultant CNC and CNF with high thermal stability and a large aspect ratio are excellent for bio-composite applications.

Introduction

Cellulose is a renewable natural polymer and can be sustainably produced from lignocellulosic plant biomass that is available in large quantities in many regions of the world. Worldwide annual production of cellulose is approximately 75 to 100 billion tons.[1,2] Cellulose nanomaterials such as cellulose nanocrystals (CNC) have attracted great attention recently due to their unique mechanical and optical properties[3–6] with potential to produce a variety of renewable and biodegradable products for a sustainable future.[7,8] Economic and environmentally sustainable production of CNC, however, is the key aspect to achieve these potentials.

Currently, CNC is mainly produced by acid hydrolysis of non-crystalline cellulose using concentrated mineral acids[9–14] which was developed in the 1940s and 1950s.[15–18] The main concerns with using mineral acid hydrolysis are: (1) the difficulties in economic acid recovery (approximately 9 kg H_2SO_4 per kg CNC using sulfuric acid) and the requirement for disposal of a large amount of salt (approximately 13 kg Na_2SO_4 per kg CNC) from acid neutralization; (2) the low thermal-stability of the resultant CNC, especially when sulfuric acid is used due to the presence of sulfate groups[19] though sodium exchange can increase the thermal stability to that of the feedstock cellulose, which limits CNC application to a very large market of nanocomposites processed at relatively high temperatures; (3) the difficulties in functionalization of CNC due to the presence of sulfate groups from sulfuric acid; and (4) low CNC yield of approximately 30–50% reported by most literature studies and pilot plant operations under the so called standard hydrolysis conditions (64 wt% acid concentration at 45–50 °C for approximately 60 min). Recent studies in our laboratory indicated that acid concentration was a critical parameter in dictating the CNC yield and morphology.[10,20] CNC yield of 75% was achieved using a bleached kraft eucalyptus pulp with a cellulose content of approximately

[a]*State Key Lab Pulp and Paper Eng., South China University of Technology, Guangzhou, China 510640*
[b]*Forest Products Laboratory, U.S. Forest Service, U.S. Department of Agriculture, Madison, WI 53726, USA. E-mail: jzhu@fs.fed.us*
[c]*Southern Research Station, U.S. Forest Service, U.S. Department of Agriculture, Auburn, Alabama 36849, USA*
†Electronic supplementary information (ESI) available. See DOI: 10.1039/c6gc00687f

80%. Overall, CNC production using concentrated mineral acid hydrolysis remained environmentally unsustainable, very expensive, and economically out of reach for most product development applications.

Enzymatic hydrolysis is environmentally friendly and was also employed together with mechanical fibrillation to produce CNC,[21] however, the isolation of CNC from a mixture of cellulose fibrils with large variation in size after mechanical processing needs to be demonstrated. Furthermore, a substantial amount of mechanical energy is required to disintegrate enzymatically hydrolyzed cellulose fibers into nanofibrils or nanocrystals.[22,23] In addition, the resultant CNC is difficult to disperse and functionalize. The thermal stability of enzymatic CNC is limited to that of the feed fibers.

Current knowledge on cellulose ultrastructure suggests that acid hydrolysis is the only pathway for producing CNC by hydrolysis of the non-crystalline cellulose. Oxidation chemistry was, however, also applied to produce rod-like cellulose nanoparticles that were also termed CNC.[24,25] Oxidation resulted in CNC with reduced thermal stability.[26] Furthermore, chemical recovery is not possible as oxidants are consumed. Moreover potential toxic compounds may be produced through the reactions of the oxidants with lignocellulosic components. Because of the low solid loading for oxidation reactions, a substantial amount of waste water needs to be treated.

Solid acids have been used to hydrolyze cellulose for sugar production with the advantage of easing acid recovery.[27–29] Recently, phosphotungstic acid was used to produce CNC with good yield but a very long reaction time of 30 h was required.[30] Furthermore, the resultant CNC was not functionalized, with low surface charge and therefore poor dispersion. The thermal stability was the same as that of the feed fibers. In the current study we use a selective category of solid organic acids to produce CNC through hydrolysis. These organic acids have low water solubility at ambient temperatures and therefore can be crystallized for low cost acid recovery, but are highly soluble at elevated temperatures resulting in effective hydrolysis of hemicelluloses and depolymerization of cellulose at high concentrations. When using certain dicarboxylic acids, the hydrolyzed cellulosic materials can be functionalized with carboxyl groups as shown in Fig. 1, through Fischer–Speier esterification[31] of one carboxyl group. This differs from reported studies using acetic or butyric acid (single carboxylic acids) hydrolysis that produced only esterified, but not carboxylated, cellulose nanowhiskers through subsequent mechanical agitation[32] or ultrasonication[33] with the assistance of a mineral acid. Cellulose esterification by poly-carboxylic acids is well known for cellulose crosslinking.[34] Moreover, Allen and Cuculo[35] provided a comprehensive review on forming semi-acid ester (or carboxylation) rather than crosslinked cellulose using poly-carboxylic acids. The focus of the past work reported in the review, however, was on enhancing crosslinking and reducing cellulose depolymerization or degradation using catalysts for textile applications.

We hypothesized that a certain degree of cellulose depolymerization or degradation can be beneficial for producing

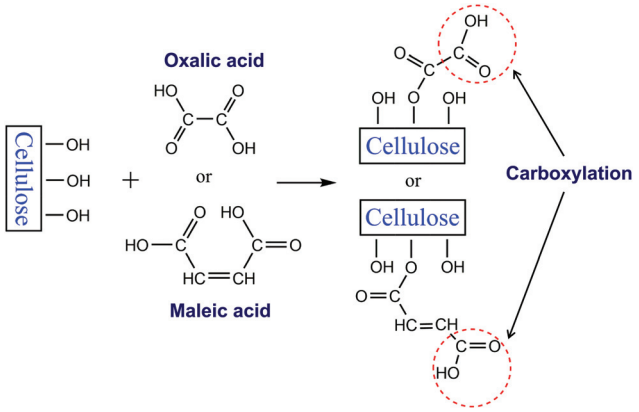

Fig. 1 A schematic diagram shows cellulose carboxylation by dicarboxylic acids through esterification of one carboxyl group.

cellulose nanomaterials without affecting the performance properties of end products, contrary to applications in textiles. We, therefore, can conduct simple hydrolysis reactions using dicarboxylic acids for producing carboxylated CNC without employing complex chemistry, such as salts, catalysts, or solvents,[35] to inhibit cellulose depolymerization. The selection of carboxylic acids, however, needed to meet certain criteria, *i.e.*, solid acid for promoting acid recovery, and moderate acid strength ($pK_a \approx 1.0$–3.0) for effective hydrolysis of hemicelluloses and non-crystalline cellulose and depolymerization of cellulose. High acid concentrations were used to minimize cellulose crosslinking[36] while enhancing esterification and therefore maximizing carboxylation, and to allow acid recovery and reactions being conducted under non-boiling conditions without using pressure vessels.

Mineral acids were not used in the present study to avoid complication. Only a small fraction of cellulose was hydrolyzed to CNC as expected due to the lower strength of organic acids compared to mineral acids such as sulfuric acid, with a majority of cellulose remaining as partially hydrolyzed fibrous cellulosic solid residue (FCSR). However, FCSR can be used to produce cellulose nanofibrils (CNF), another kind of cellulose nanomaterials, through subsequent mechanical fibrillation, to achieve integrated production of CNC with CNF as we demonstrated previously using sulfuric acid.[9,37] Furthermore, the yield and morphologies of CNC and CNF can be tailored by controlling reaction severity (*e.g.*, acid type, concentration, reaction temperature and time) and the intensity of subsequent mechanical fibrillation. The overall solid yield (CNC + CNF) was very high. Only hemicelluloses were hydrolyzed to sugars that can also be recovered as they are not crystallized with acid.

Results and discussion

CNC and CNF yields

The recyclable organic acid hydrolysis (ROAH) approach used in this work is schematically presented in Fig. 2. Acid

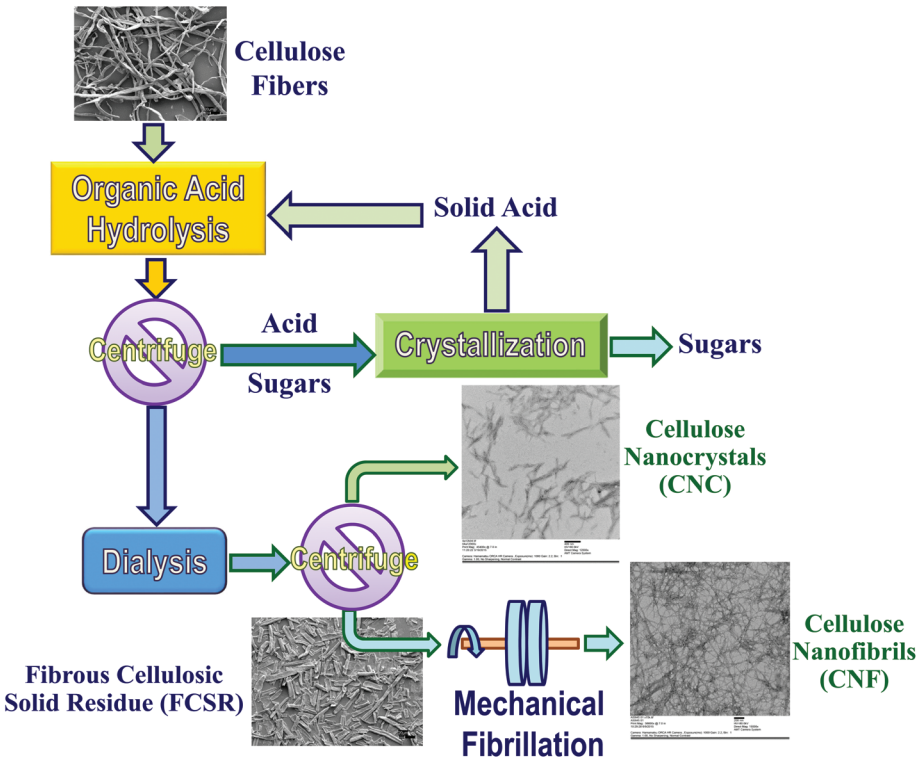

Fig. 2 A schematic flow diagram of experiments for integrated CNC and CNF production with recovery of organic acids.

hydrolysis experiments on a bleached kraft eucalyptus pulp (BEP) were carried out over a range of acid concentrations (30–80 wt%), hydrolysis temperature (80–120 °C) and time (30–240 min) using oxalic (O), maleic (M), and *p*-toluenesulfonic (T) acids. The chemical composition of BEP was glucan 78.1 ± 1.0%, xylan 15.5 ± 0.6%, and Klason lignin 0.1 ± 0.1%.[22] The yields of CNC and FCSR along with reducing sugar recovery from these experiments are listed in Table S1 (ESI†). The reducing sugar recovery was measured using the DNS assay of the hydrolysates.[38] Xylose was the major sugar for runs under low severity (short time) hydrolysis conditions as revealed from HPLC analyses of selected hydrolysates (Table S1†), suggesting that glucan dissolution was minimal. The results suggest that xylan solubilization was substantial under most of the hydrolysis conditions, *e.g.*, more than 60% of the xylan were hydrolyzed at an acid concentration of 60 wt% or higher or a reaction time over 60 min at 100 °C or higher using oxalic acid. The low glucan dissolution (<10%) was also corroborated by the high yield of total solids (CNC + FCSR). CNC yield was low with the highest yield of approximately 25% due to insufficient hydrolysis[9,20] because the dicarboxylic acids are weaker (pK_a = 1.25 and 1.9 for oxalic and maleic acid, respectively) than mineral acids such as sulfuric acid (pK_a = −3.0). The run using *p*-toluenesulfonic acid, a strong organic acid (pK_a = −2.8), was conducted at a low acid concentration of 50 wt% (even lower in molar base compared with the lower molecular weight of sulfuric acid) to achieve sufficient hydrolysis. Our previous studies indicated that a sulfuric acid concentration of 56 wt% is the critical point to achieve sufficient hydrolysis for high yield of CNC.[10,20]

CNC and CNF morphology

To facilitate discussion, the CNC and CNF samples are labelled using abbreviated hydrolysis conditions as (Axx, xxx, xx) to represent acid (A = O for oxalic; = M for maleic; = T for *p*-toluenesulfonic; = B as benzenesulfonic acid) loading in wt%, reaction temperature in °C, and duration in min. In general, CNC was produced as revealed by AFM topographic images (Fig. 3a–d) using oxalic acid under several conditions. The AFM images clearly showed good CNC dispersion. The diameters of the CNC were approximately 15 nm. Fiber bundles or crystal aggregates can be clearly seen from the 15 μm scans (top panel of Fig. 3) due to the weak acidity of oxalic acid, especially at low acid loading of 50 wt% (Fig. 3a). Increasing acid loading and reaction time improved crystal separation with more uniform CNC particle diameters (Fig. 3b–d). Furthermore, increasing centrifuge speed can also reduce aggregates in the accepted CNC with reduced yield. However, the rejected aggregates can be subsequently fibrillated to CNF. AFM topographic measurements of crystal heights were used as CNC diameters, which confirmed the improved separation of crystal aggregation (Fig. 4). The number averaged CNC particle lengths were 377 nm, 290 nm, 278 nm, and 273 nm for the four CNC samples shown in Fig. 3a–d, respectively, as determined by image analyses (Image J 1.47 v, National Institute of Health, USA) through randomly picking approximately 70 CNC particles for each sample. These

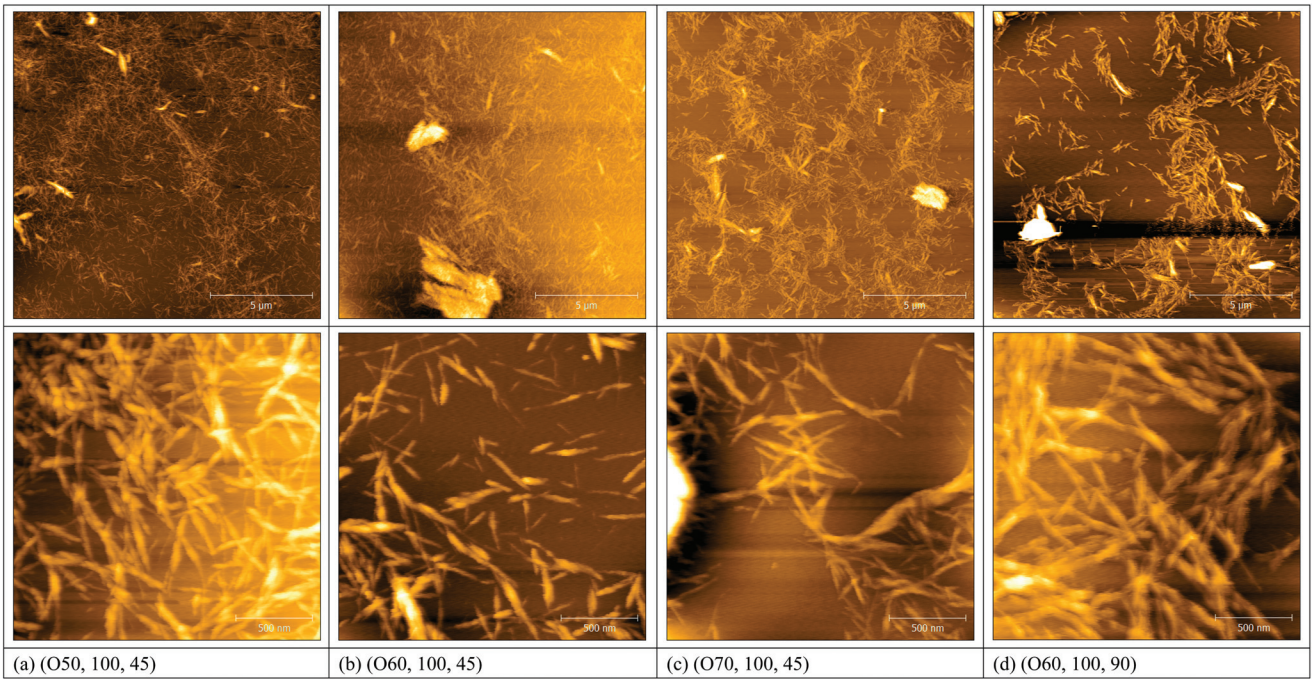

Fig. 3 AFM topographic images of the CNC samples produced under various oxalic acid hydrolysis conditions. Scale = 5 µm, 500 nm in the top and bottom panel, respectively. (a) (O50, 100, 45); (b) (O60, 100, 45); (c) (O70, 100, 45); (d) (O60, 100, 90).

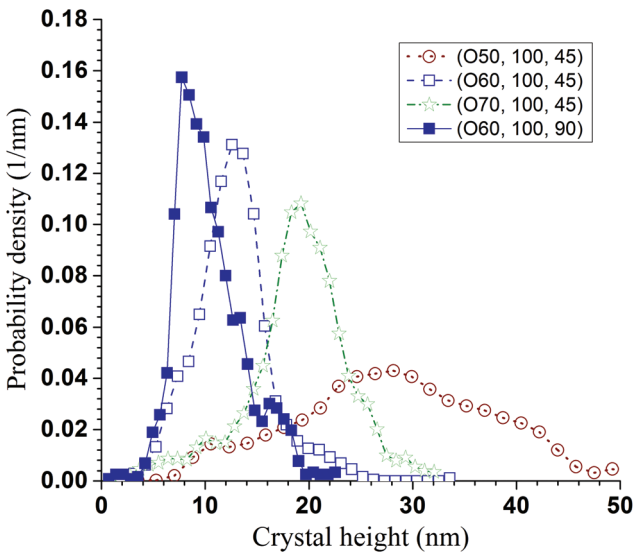

Fig. 4 Probability density distributions of AFM topography measured heights of the CNC samples shown in Fig. 3.

CNC lengths are longer than the conventional sulfuric acid produced CNC under standard conditions.[10] Increased hydrolysis severity reduced average CNC length. Based on these measured averaged CNC lengths and heights, the average CNC aspect ratios were 13.4, 22.8, 14.6, and 27.3, respectively, for the four samples shown in Fig. 3a–d.

Subsequent mechanical fibrillation of various partially acid hydrolyzed FCSR samples using microfluidization produced CNF with varied morphologies as shown in Fig. 5a–c. The morphology of the CNF from the FCSR resulting from acid hydrolysis at low acid concentration of 50 wt% was a slightly entangled fibril network (Fig. 5a). The number averaged fibril lengths and diameters were 1096 and 8.5 nm, 624 and 5.1 nm, 481 and 5.2 nm, respectively, for the three samples shown in Fig. 5a–c based on similar measurements for CNC described above. Increasing acid concentration or reaction severity resulted in CNF as individual fibrils with short lengths and diameters (Fig. 5b and c). This suggests that acid hydrolysis substantially facilitated mechanical fibrillation of the resultant FCSR due to the reduced degree of polymerization (DP). The DP of the FCSR samples corresponding to the CNF samples shown in Fig. 5a–c measured by a TAPPI Standard method (TAPPI T230 om-08) were 287, 265, and 239, equivalent to molecular weights of approximately 46 460, 42 880, and 38 730, respectively. Hydrolysis at (O70, 100, 45) may have over hydrolyzed BEP to a low DP of 239 to result in shorter CNF whisker like particles with an average length of 480 nm (Fig. 5c). This also suggests that fewer passes in microfluidization or energy input than used here are needed. These whisker-like CNF may be called CNC as reported in some literature.[21] In this way, we can produce chemical (acid hydrolysis)-mechanical CNC (AHM-CNC) such as shown in Fig. 5c under severe acid hydrolysis and fibrillation conditions. However, the aspect ratio L/D for the sample shown in Fig. 5c is 93, substantially greater than those of the CNC shown in Fig. 3a–d.

The results shown in Fig. 5a–c suggest that a low reaction severity, *i.e.*, lower acid concentration or temperature along with milder mechanical fibrillation can produce longer fibrils

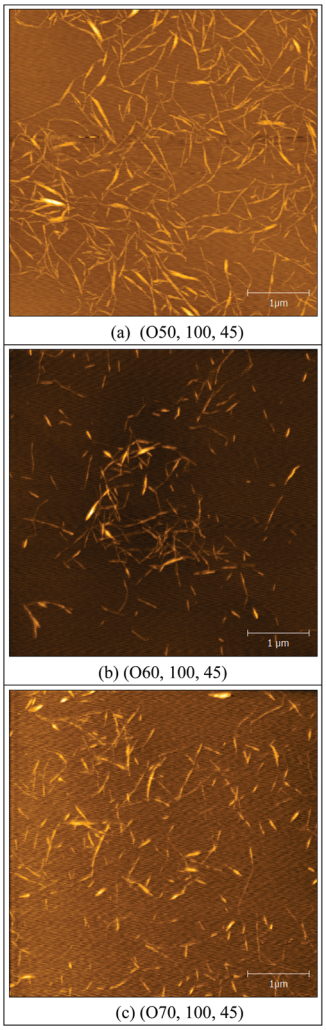

Fig. 5 AFM topographic images of the CNF samples produced from FCSR under various oxalic acid hydrolysis conditions. Scale = 1 μm. (a) (O50, 100, 45); (b) (O60, 100, 45); (c) (O70, 100, 45).

as shown in Fig. S1.† CNC was undetectable with near 100% FCSR yield under low severity hydrolysis conditions (Table S1†); therefore, the process ends up producing only CNF with long fibril lengths. One can use acid hydrolysis severity factors, such as the combined hydrolysis factor (CHF) that has been shown to correlate to hemicellulose dissolution,[39–41] to correlate CNF length or strength properties for process control.

Thermal stability

Thermogravimetric analyses (TGA) of the CNC, CNF, and the original BEP fibers were conducted using a Pyris 1 TGA (Perkin-Elmer, Inc., Waltham, MA) with temperatures from ambient to 600 °C at a heating rate of 10 °C min^{-1}. Approximately 5 mg of sample were used for each test. Samples were first dried at 50 °C for 4 h prior to testing. A high purity nitrogen stream with a flow rate of 20 mL min^{-1} was continuously passed into a furnace before thermal decomposition was carried out to prevent any unwanted oxidative decomposition. The reported weight loss was normalized against the initial weight. The results clearly show (Fig. 6a and b) that the CNC samples produced using oxalic, maleic, *p*-toluenesulfonic, and benzenesulfonic acids at (O70, 100, 60), (M60, 100, 45), (T50, 100, 45), and (B50, 100, 45), respectively, had substantially higher thermal stability than those produced using mineral acids such as sulfuric (S), phosphoric (P), and hydrochloric (H) acids under standard conditions[10,12–14,42] of (S64, 45, 45), (P67, 100, 45), and (H14, 100, 45), respectively. The onset thermal degradation temperature can be defined when $dW/dT \geq -1$, *i.e.*, where weight loss is greater and equal to 1% with an increase in temperature of 1 degree. The CNC (O70, 100, 60) had the

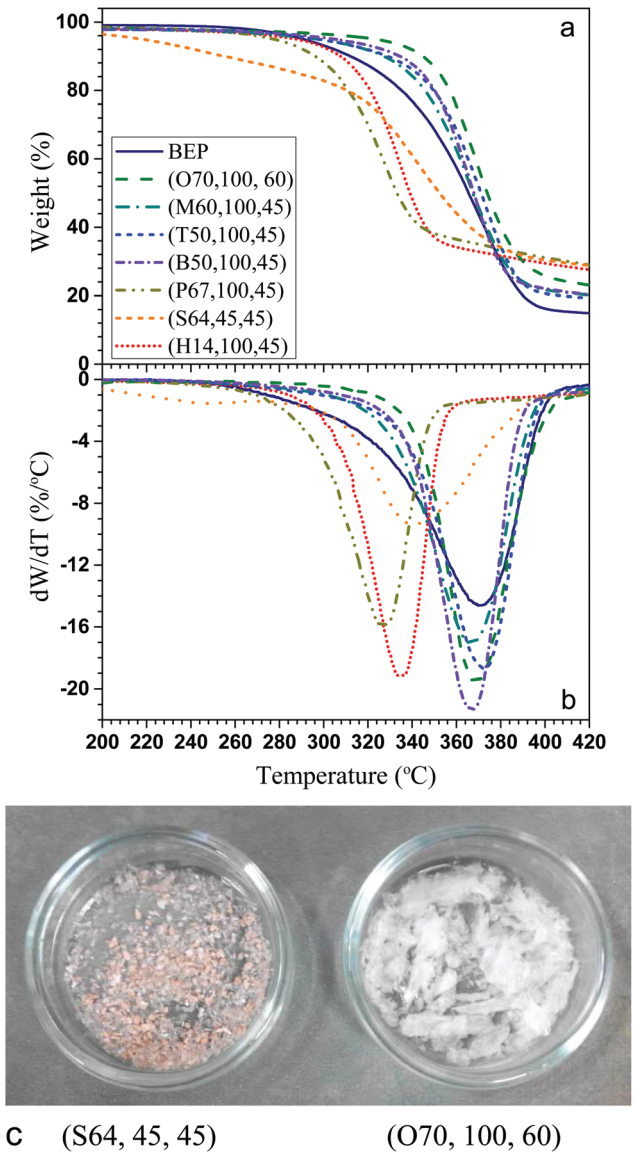

Fig. 6 Comparisons of thermal stability of different CNC samples produced under various acid hydrolysis conditions. (a) TGA weight loss; (b) TGA temperature derivative weight loss; (c) the color of two CNC samples from sulfuric and oxalic acid hydrolysis after 4 h in an oven at 105 °C.

highest onset thermal degradation temperature of approximately 322 °C, compared with 274 °C for the original BEP fibers, and 218 °C for (S64, 45, 45), or the onset degradation temperature T_{onset} of (O70, 100, 60) is at least 100 °C higher than that of (S64, 45, 45). The T_{onset} and the corresponding weight loss along with T_{95} at 5% weight loss of all the CNC samples produced were also compared (Table S2†). The comparisons clearly demonstrate the greater thermal stability of the CNC samples produced with the four organic acids, a significant advantage for thermal processing such as extrusion at high temperatures.

To further demonstrate the thermal stability of the CNC produced by the present ROAH, CNC samples from (O70, 100 60) and (S64, 45, 45) were tested in an oven at 105 °C for 4 h. (S64, 45, 45) was rapidly degraded as shown by the orange color of the sample while (O70, 100, 60) remained in the original white color (Fig. 6c).

Interaction with water and surface charge

Aqueous suspensions of the CNC samples were evaluated with time domain ^{1}H NMR analyses using a Bruker mq20-Minispec, with a 0.7 Tesla permanent magnet (20 MHz proton resonance frequency), operating at 40 °C. The transverse ($T2$) relaxation times were determined using the Carr–Purcell–Meiboom–Gill (CPMG) sequence. 8000 echoes were collected with a pulse separation of 0.7 ms, the acquisition of 32 scans and a 5 s recycle delay. The inverse Laplace transform method CONTIN, was used to determine relaxation time distributions. The results indicated that all samples had one peak corresponding to interaction between CNC with water. However, the relaxation time $T2$ for different samples was different as shown in Table 1. Pure water had a $T2$ of approximately 2000 ms. This clearly indicates that the sulfuric acid produced CNC (S64, 45, 45) had the strongest interaction with water with a very low $T2$ of approximately 1300 ms, *i.e.*, highly hydrophilic. The CNC from hydrochloric acid (H15, 100, 45) and phosphoric acid (P67, 100, 45) both had very limited interactions with water having a $T2$ over 1900 ms. All of the oxalic acid produced CNC samples had some interactions with water and were hydrophilic but not as strongly as (S64, 45, 45). This can be beneficial for many applications such as facilitating water removal and improving moisture barrier properties. The weak interaction with water supports the improved thermal stability discussed above.

The surface charges of the CNC samples were measured using a zeta potential analyzer (Nanobrook Omni, Brookhaven Instruments, Holtsville, NY) based on monitoring electrophoretic mobility using Phase Analysis Light Scattering (PALS). The method was developed for spherical particles, but an approximation for rod-like cellulose nanoparticles was used in this study. The surface charges provided good dispersion in water due to electrostatic repulsion as shown by the AFM images of the samples (Fig. 3a–d). In general, increasing acid loading in hydrolysis increased surface charge (absolute value) as shown in Table 1. CNC samples produced using oxalic acid were just as highly charged as the CNC produced using sulfuric acid under standard conditions (S64, 45, 45). Maleic acid, however, produced lower charge than oxalic acid under the same reaction conditions, perhaps due to the weak reactivity in esterification with cellulose OH groups. However, the charge was still higher than CNC produced using phosphoric and hydrochloric acids.

Table 1 NMR relaxation time $T2$, surface charge, carboxyl group content, and crystallinity index CrI of the CNC samples

CNC sample	NMR relaxation time $T2$ (ms)	CNC Charge (mV)	COOH (mmol per g CNC)	CrI (%)
BEP			ND	76.0 ± 0.4
(O50, 100, 45)		−38.0 ± 0.3	0.11	82.8
(O60, 100, 45)	1692	−41.9 ± 0.7	0.15	82.4
(O70, 100, 45)	1772	−43.3 ± 0.9	0.19	81.2
(O50, 100, 90)	1622	−38.7 ± 0.6	0.17	81.3
(O60, 100, 90)		−45.0 ± 0.3	0.39	80.0
(O70, 100, 60)	1630	−42.5 ± 0.5	0.23	80.4
(M50, 100, 45)		−30.1 ± 0.4		
(M60, 100, 45)		−31.3 ± 0.2		
(M70, 100, 45)		−33.3 ± 0.7		
(T50, 100, 45)		−20.7 ± 0.5		82.4
(S64, 45, 45)	1333	−59.4 ± 0.8		77.9 ± 0.2
(P67,100, 45)	1960	−23.0 ± 0.6		
(H14, 100, 45)	1954	−21.9 ± 0.7		

Esterification and carboxylation

Fourier transform infrared (FT-IR) absorption of two CNC samples, (O70, 100, 45) and (M60, 100, 45) along with the original BEP fibers were analyzed using a FT-IR spectrophotometer (Spectrum 100, PerkinElmer, Waltham, MA) equipped with a universal attenuated-total-reflection (ATR) probe. As shown in Fig. 7, several absorption peaks were observed. The identifications of these peaks are listed in Table S3.† The main feature of the two CNC samples is esterification as observed from the ester carbonyl groups (C═O) at 1737 cm^{-1} that does not appear in the original BEP sample (see the insert plot in Fig. 7). This suggests that one of the carboxyl groups in the oxalic and maleic acids reacted with cellulose (most likely at C6 position[36]) to form ester groups on CNC. However the peak at 1737 cm^{-1} was not very strong from either sample, suggesting moderate degrees of esterification.

Conductometric titration of the CNC samples was conducted to quantify cellulose carboxylation through esterification by dicarboxylic acid (Fig. 1) using a conductance meter (YSI Model 35, Yellow Springs Instrument Co., Ohio, USA). A small volume of a suspension containing 50 mg CNC or CNF was added to 1 mM NaCl solution (about 120 mL) and titrated using 2 mM NaOH by adding approximately 0.2 mL in 30 second intervals. An initial decrease in conductivity was observed as the protons associated with the carboxyl group were consumed. Then, conductivity was increased once all the hydrogen ions had been neutralized with added NaOH. The amount of carboxyl groups was calculated based on the consumed NaOH relative to the inflection point. The results indicate that the carboxyl group content ranged from

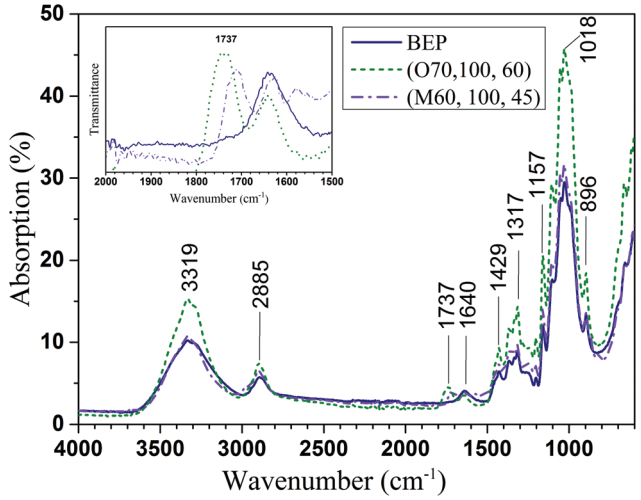

Fig. 7 FTIR absorption spectra of two CNC samples from oxalic and maleic acid hydrolysis compared with that of the original BEP fibers.

0.11–0.39 mmol per g CNC for the 6 CNC samples produced using oxalic acid (Table 1). The carboxylation of CNC can provide various chemical reaction pathways to achieve different functional properties.

Crystallinity

The crystallinity indices (CrI) of selected CNC samples were analyzed using wide-angle X-ray diffraction on a Bruker D8 130 Discover system with Cu-Kα radiation (Bruker Corp., Billerica, MA, USA). As described previously,[10] the Segal method[43] (without base line subtraction) was used to determine CrI. The results indicate that the CrI of CNC samples from concentrated oxalic acid hydrolysis were approximately 81% (Table 1), compared with 76% for the original BEP fibers and 78% for the CNC produced by sulfuric acid under standard conditions (S64, 45, 45). The variation of CrI under hydrolysis conditions in the range studied was minimal. The CNC from *p*-toluenesulfonic acid (T50, 100, 45) also has a high CrI of 82.4%. The higher CrI of ROAH derived CNC may explain their higher thermal stability than that of CNC from sulfuric acid.

Acid recovery

Substantial crystallization of oxalic acid in hydrolysates that were cooled to ambient temperature was observed even with a three-fold dilution of the hydrolysate at 80 °C (Fig. S2†). Oxalic acid recoveries from hydrolysates under different reaction conditions were experimentally quantified. An aliquot of hot hydrolysate was sampled from each of the 6 oxalic acid hydrolysis runs before cooling. After crystallization at 20 °C, the measurable liquid volume of the hydrolysates was negligible. The impurity in the hydrolysate promoted crystallization. Furthermore, water was absorbed to the acid crystals to form an acid-hydrate that substantially reduced the solution volume. Therefore, we can assume that there is no soluble acid or 100% crystallization. The sampled hot hydrolysates were directly analyzed before crystallization using UV absorption described in the ESI.† As listed in Table 2, the amounts of oxalic acid remaining in the hot hydrolysates that were crystallized after cooling were approximately 95% for all 6 experiments under different acid concentrations.

Table 2 Recovery of oxalic acid from real hydrolysates of BEP compared with the corresponding calculated recoveries based on acid solubility in aqueous solutions

Hydrolysis conditions	Hydrolysate (%)	Calculated (eqn (S2))
(O50, 100, 45)	96.0 ± 1.3	90.9
(O50, 100, 90)	95.9 ± 0.1	90.9
(O60, 100, 45)	96.3 ± 0.8	93.9
(O60, 100, 90)	95.9 ± 0.5	93.9
(O70, 100, 45)	95.4 ± 0.3	96.1
(O70, 100, 60)	94.5 ± 0.2	96.1

Conclusions

This study demonstrated the production of cellulose nanomaterials, such as cellulose nanocrystals (CNC) and fibrils (CNF), with excellent thermal stability by concentrated acid hydrolysis using recyclable solid organic acids at ambient pressure. When using certain dicarboxylic acids, cellulose can be esterified by one carboxyl group of the dicarboxylic acid to result in carboxylated CNC and CNF, important for functionalization. The recyclability of acid through simple crystallization using solid acids, surface functionality through carboxylation, and improved thermal stability of the resultant CNC and CNF, makes green and sustainable production of renewable cellulose nanomaterial possible for a variety of high value applications. Therefore, the present study has significant practical importance.

Experimental

Materials

Sulfuric, hydrochloric, phosphoric, anhydrous oxalic, and anhydrous maleic acids, *p*-toluenesulfonic, and benzenesulphonic acids were purchased from Sigma-Aldrich (St. Louis, MO). The densities of different organic acid solutions at 100 °C were measured as shown in the ESI (Fig. S3†). The density variation with temperature was negligible.

A bleached kraft eucalyptus dry lap pulp (BEP) was obtained from a commercial source (Fibria, Aracruz Celulose, Brazil). The dry lap was soaked in water overnight and disintegrated using a disintegrator (Model 73-06-01, TMI, Ronkonkoma, New York, USA) for 10 000 revolutions at 3120 rpm and 2% consistency at room temperature. The pulp was then vacuum dewatered and air dried to an approximately 5% moisture content.

CNC and CNF production

Concentrated aqueous acid solutions were prepared by heating a desired amount of DI water in a multiple-neck flask in a

liquid glycerol bath on a heating plate to approximately 80 °C. An appropriate amount of the selected anhydrous organic acid was added to make a solution of desired concentration with the aid of magnetic stirring. The solution temperature can be raised to the desired hydrolysis temperature between 90 and 120 °C without boiling at high acid concentrations. The density data shown in Fig. S3† were used to determine the required amounts of water and the acid to make a concentrated acid solution of 80 mL at a given acid mass concentration. BEP fibers of 10 g in oven dry (OD) weight were added into the acid solution with continuous stirring. At the end of the set reaction time, an aliquot of the acid hydrolysate was taken for acid recovery and sugar analyses. The reaction was then terminated by adding 160 mL of 80 °C DI-water to avoid crystallization (iced water can be used to minimize dilution water usage while effectively terminating the reaction). The resultant suspension was quickly filtered using filter paper under vacuum to separate the solids (CNC and FCSR) from the organic acid solution. The filtrate was then crystallized for reuse. The filtered solids were diluted with water for washing and then centrifuged at 2603*g* (higher centrifuge speed can be used to improve separation) for 10 min. The supernatant was decanted off, fresh water was added to the solids and mixed. This washing and centrifuging procedure was repeated until the supernatant was turbid, indicating that CNC were being dispersed into solution. The turbid supernatant and settled solids (FCSR) were then mixed together and this slurry was dialyzed using DI-water until the conductivity of the liquid approached that of DI-water, indicating near-complete acid removal. The CNC dispersion was finally obtained by centrifuging the dialyzed sample at 2603*g* for 10 min to separate FCSR from CNC which stayed in the aqueous phase. The amount of CNC in the dispersion was measured using a COD method described previously[9,20] to determine CNC yield.

To recover solubilized sugars in the acid hydrolysate, the liquid hydrolysates after acid crystallization were settled in the sealed glass bottle overnight to cool to ambient temperature. The acid crystals were separated from liquid hydrolysate by vacuum filtration. The soluble sugar can then be recovered after neutralizing the remaining acid in the liquid hydrolysate. With optimization, the remaining acid in the final liquid hydrolysate can be kept at minimum to reduce acid loss.

The precipitated FCSR were quantified using the gravimetric method for yield determination. The FCSR was then mechanically fibrillated at 1 wt% concentration in water using a microfluidizer (Microfluidizer M-110EH, Microfluidics Corp., Westwood, MA) to produce CNF. The fiber suspension was first passed through a 200 μm chamber for 5 passes at 5 MPa, and then additional 5 passes through an 87 μm chamber at 130 MPa, respectively.

Acknowledgements

This work was conducted while Chen was a visiting Ph.D. student at the US Forest Service, Forest Products Laboratory (FPL), Madison, WI, and on official government time of Zhu, Baez, and Elder. This work was partially supported by the USDA Agriculture and Food Research Initiative (AFRI) Competitive Grant (no. 2011-67009-20056), Guangzhou Elite Project of China. Funding from these programs made the visiting appointments of Chen at FPL possible.

References

1 A. D. French, N. R. Bertoniere, R. M. Brown, H. Chanzy, D. Gray, K. Hattori and W. Glasser, in *Kirk-Othmer Encycl. Chem. Technol*, ed. A. Seidel, John Wiley & Sons, Inc., New York, 5th edn, 2004, vol. 5.
2 M. M. de Souza Lima and R. Borsali, *Macromol. Rapid Commun.*, 2004, **25**, 771–787.
3 J.-F. Revol, L. Godbout, X.-M. Dong, D. G. Gray, H. Chanzy and G. Maret, *Liq. Cryst.*, 1994, **16**, 127–134.
4 X. M. Dong and D. G. Gray, *Langmuir*, 1997, **13**, 3029–3034.
5 Y. Habibi, L. A. Lucia and O. J. Rojas, *Chem. Rev.*, 2010, **110**, 3479–3500.
6 R. J. Moon, A. Martini, J. Nairn, J. Simonsen and J. Youngblood, *Chem. Soc. Rev.*, 2011, **40**, 3941–3994.
7 J. A. Kelly, A. M. Shukaliak, C. C. Y. Cheung, K. E. Shopsowitz, W. Y. Hamad and M. J. MacLachlan, *Angew. Chem., Int. Ed.*, 2013, **52**, 8912–8916.
8 M. Giese, L. K. Blusch, M. K. Khan and M. J. MacLachlan, *Angew. Chem., Int. Ed.*, 2015, **54**, 2888–2910.
9 Q. Q. Wang, J. Y. Zhu, R. S. Reiner, S. P. Verrill, U. Baxa and S. E. McNeil, *Cellulose*, 2012, **19**, 2033–2047.
10 L. Chen, Q. Wang, K. Hirth, C. Baez, U. P. Agarwal and J. Y. Zhu, *Cellulose*, 2015, **22**, 1753–1762.
11 D. Bondeson, A. Mathew and K. Oksman, *Cellulose*, 2006, **13**, 171–180.
12 W. Y. Hamad and T. Q. Hu, *Can. J. Chem. Eng.*, 2010, **88**, 392–402.
13 H. Yu, Z. Qin, B. Liang, N. Liu, Z. Zhou and L. Chen, *J. Mater. Chem. A*, 2013, **1**, 3938–3944.
14 S. Camarero Espinosa, T. Kuhnt, E. J. Foster and C. Weder, *Biomacromolecules*, 2013, **14**, 1223–1230.
15 R. F. Nickerson and J. A. Habrle, *Ind. Eng. Chem.*, 1947, **39**, 1507–1512.
16 O. A. Battista, *Ind. Eng. Chem.*, 1950, **42**, 502–507.
17 B. G. Rånby, *Discuss. Faraday Soc.*, 1951, **11**, 158–164.
18 S. M. Mukherjee and H. J. Woods, *Biochim. Biophys. Acta*, 1953, **10**, 499–511.
19 M. Roman and W. T. Winter, *Biomacromolecules*, 2004, **5**, 1671–1677.
20 Q. Wang, X. Zhao and J. Y. Zhu, *Ind. Eng. Chem. Res.*, 2014, **53**, 11007–11014.
21 S. R. Anderson, D. Esposito, W. Gillette, J. Y. Zhu, U. Baxa and S. E. McNeil, *Tappi J.*, 2014, **13**, 35–41.
22 Q. Q. Wang, J. Y. Zhu, R. Gleisner, T. A. Kuster, U. Baxa and S. E. McNeil, *Cellulose*, 2012, **19**, 1631–1643.
23 I. C. Hoeger, S. S. Nair, A. J. Ragauskas, Y. Deng, O. J. Rojas and J. Y. Zhu, *Cellulose*, 2013, **20**, 807–818.

24 A. C. W. Leung, S. Hrapovic, E. Lam, Y. Liu, K. B. Male, K. A. Mahmoud and J. H. T. Luong, *Small*, 2011, **7**, 302–305.
25 S. Montanari, M. Roumani, L. Heux and M. R. Vignon, *Macromolecules*, 2005, **38**, 1665–1671.
26 H. Fukuzumi, T. Saito, Y. Okita and A. Isogai, *Polym. Degrad. Stab.*, 2010, **95**, 1502–1508.
27 Y. B. Huang and Y. Fu, *Green Chem.*, 2013, **15**, 1095–1111.
28 K. I. Shimizu and A. Satsuma, *Energy Environ. Sci.*, 2011, **4**, 3140–3153.
29 F. Guo, Z. Fang, C. C. Xu and R. L. Smith Jr., *Prog. Energy Combust. Sci.*, 2012, **38**, 672–690.
30 Y. Liu, H. Wang, G. Yu, Q. Yu, B. Li and X. Mu, *Carbohydr. Polym.*, 2014, **110**, 415–422.
31 E. Fischer and A. Speier, *Chem. Ber.*, 1895, **28**, 3252–3258.
32 B. Braun and J. R. Dorgan, *Biomacromolecules*, 2009, **10**, 334–341.
33 L. Tang, B. Huang, Q. Lu, S. Wang, W. Ou, W. Lin and X. Chen, *Bioresour. Technol.*, 2013, **127**, 100–105.
34 C. Q. Yang and X. Wang, *Text. Res. J.*, 1996, **66**, 595–603.
35 T. C. Allen and J. A. Cuculo, *J. Polym. Sci., Part D: Macromol. Rev.*, 1973, **7**, 189–262.
36 J. C. P. de Melo, E. C. da Silva Filho, S. A. A. Santana and C. Airoldi, *Colloids Surf., A*, 2009, **346**, 138–145.
37 Q. Q. Wang, J. Y. Zhu and J. M. Considine, *ACS Appl. Mater. Interfaces*, 2013, **5**, 2527–2534.
38 G. L. Miller, *Anal. Chem.*, 1959, **31**, 426–428.
39 W. Zhu, C. J. Houtman, J. Y. Zhu, R. Gleisner and K. F. Chen, *Process Biochem.*, 2012, **47**, 785–791.
40 H. Zhou, J. Y. Zhu, X. Luo, S.-Y. Leu, X. Wu, R. Gleisner, B. S. Dien, R. E. Hector, D. Yang, X. Qiu, E. Horn and J. Negron, *Ind. Eng. Chem. Res.*, 2013, **52**, 16057–16065.
41 J. Zhang, F. Gu, J. Y. Zhu and R. S. Zalesny, *Bioresour. Technol.*, 2015, **186**, 223–231.
42 J. Araki, M. Wada, S. Kuga and T. Okano, *Colloids Surf., A*, 1998, **142**, 75–82.
43 L. Segal, J. J. Creely, A. E. Martin and C. M. Conrad, *Text. Res. J.*, 1959, **29**, 786–794.